

Optometry in the dark with the use of photoluminescent optotypes

Antonio Parretta^{1,2*}

¹Physics and Earth Sciences Department
Ferrara University

Via G. Saragat 1, 44122 Ferrara (FE), Italy

²Academy of Sciences of Ferrara

Via del Gregorio 13, 44121 Ferrara (FE), Italy

¹parretta@fe.infn.it; ²aparretta@alice.it

Enrico J.X. Chéng

Via San Giacomo 8, 44122 Ferrara, Italy

chengenrico08@gmail.com

Abstract—The use of photoluminescent stickers is widespread among people, particularly the youngest, which reproduce sky constellations on the ceilings of houses to be admired in the dark. They are also used in fixed warning systems (obstacles on the roads) or mobile ones (bicycles, motorcycles), to ward off the dangers of accidents. In this work I present the results of a series of optometric tests carried out in the dark using PL targets, tests that follow those well known in the field of optometry and carried out at light. The tests in the dark required, with regard to the morphoscopic visual acuity, the creation of tables similar to those used in light, but with a black background and with shaped PL symbols or characters, obtained cutting commercial photoluminescent sheets, or spreading a photoluminescent paint on a black cardboard. Of particular interest are the results obtained by experimenting in the dark the angle of view test and the Mariotte blind spot test, also proposing a new test obtained from the combination of these two. The aim of this work is therefore to highlight the aspects of human vision related to the condition of darkness and to compare them with those experienced in the light.

Keywords—optometry, visual acuity, luminance, photoluminescence, logMAR charts, UV-A light, Mariotte's test

I. INTRODUCTION

It was the observation of photoluminescent (PL) star stickers at night on the ceiling of my home that stimulated me to promote a study of vision in the dark using this type of light sources. It happened that, observing at a certain distance in the dark a group of previously illuminated PL star stickers, I discovered to my amazement, ignoring at that time this phenomenon, that, focusing the gaze on any star, it immediately disappeared from view, while those close to it, and present in the visual field of the eyes, remained visible. In addition, the star in question reappeared again if I moved my gaze to a nearby star, which in turn became dark (see Fig. 1). My pleasant surprise was only the result of my gaps in the functioning of human eye, and

this prompted me to fill them and deepen the origin of this phenomenon [1, 2].

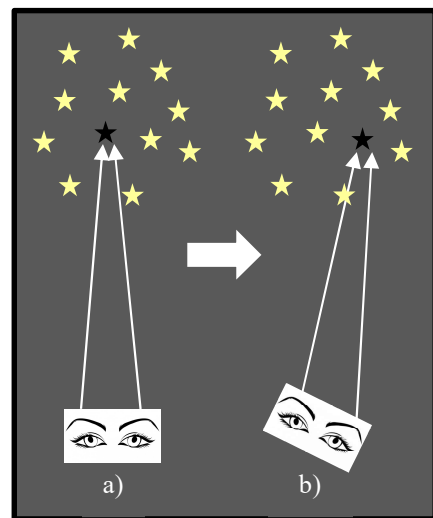


Fig. 1. Schematic representation of a ceiling covered by a group of photoluminescent star stickers. If we fix a photoluminescent star sticker, previously illuminated by white or UVA light, with eyes adapted to the dark, the sticker disappears from view (a). The same thing happens by moving the view on another sticker (b). Of course, the eyes-sticker distance must be appropriate (see after in the text).

The disappearance from view of the photoluminescent star sticker is simply due to the formation of a shadow cone, with a linear opening of $\sim 1^\circ$, that our eye projects in front of it due to the deactivation of the cones in the dark and the absence of rods in the foveal area involved by the direct view of a light source. The first test in the dark was done, therefore, to understand the phenomenon of the disappearance of a PL star sticker. This test, called "test of the angle of view", is intrinsically linked to the condition of darkness, and therefore has no equivalent to those carried out in the light. The other tests considered in this paper were performed both in the dark and in the light. To summarize, four tests will be described in this work in order of presentation:

- A) The morphoscopic acuity test (recognition acuity).
- B) The test of the angle of view.
- C) The blind spot test of Mariotte.

D) The test of resolution acuity or minimum angle of resolution.

The marks used for the various tests in the dark, in positive contrast (black background), were made using photoluminescent stickers or paints. The marks used for the various tests in the light, in positive or negative contrast, were made using white paints, or projecting them by a monitor screen. All tests are accompanied by luminance measurements of the marks and/or their background, and of the environment with a luxmeter. The lighting in the dark of the PL marks is carried out with UV-A light, while in the light the marks are illuminated with normal white light lamps or sunlight. As will be evident when reading this paper, the realization of this work required only a few commercial materials and low-cost instrumentation, which makes it very suitable to be repeated by students who want to deepen not only the art of optometry, but also the knowledge of human eye, which is the most sophisticated sense organ we have: if comparing neural input, the cochlear division of the acoustic nerve contains ~31,000 neurons, against the 1,200,000 ones of the optic nerve. The main literature references followed on visual acuity and optometry is in [1-2].

II. EXPERIMENTAL SECTION

A. Materials and instrumentation

PL stickers are made from light green vinyl adhesive tapes. The PL paint is also light green, and is sold by the company SpaceBeams. For the excitation of the stickers and PL paint with UV-A light, Wood lamps with LED source were used, the first one of the YOUTHINK company, with $\lambda = 395\text{nm}$, mod. YT-UL03, and the second one, with $\lambda = 365\text{nm}$, of the company Alonefire, mod SV53 15W. The use of UV-A lamps is always done by protecting the operator and the people present in the laboratory with UVEX i-vo glasses. The LUTRON LX-1108 luxmeter was used for luminance measurements of optotypes and their background, and for illuminance measurements on surfaces. The sensor of the luxmeter has a dome with a diameter of 21.5mm, and area $A_d=363\text{mm}^2$. The digital laser BOSCH PLR 50 C was used for optical distance measurements. Although the materials and instrumentation used are easy to acquire and cost-effective, much manual work was required for the preparation of the optotypes tables. In fact, lacking of a series of normographs covering the entire range of font sizes (factor 20), all optotypes were drawn manually. The white characters were drawn by using white paint pencils, the PL ones were drawn by brush and PL paint. Moreover, for the preparation of the logMAR tables to test the morphoscopic acuity, being particularly difficult to prepare the smallest optotypes, those relative to highest visual acuity (VA), by using painting methods, it was decided to operate at a high distance of 6m, to have the smallest characters with height of ~5mm. Furtherly, being difficult to have 6m indoor distance, a mirror was interposed between the observer and the chart, having so an optical path of 3+3m, compatible with a small environment. The use of a mirror naturally involves the drawing of inverted

characters on the chart. The optometric charts were prepared as follows. The base of the chart is a large black card (70x50cm). The chart cannot be drawn directly on it. Then, individual parts of it, already prepared on the computer with the correct dimensions, are printed on sheets of transparent A4 paper; these are then turned over and new sheets of transparent paper are placed on them. Finally, on this paper the white or the photoluminescent characters are painted by a brush, and will obviously appear inverted (left exchanged with right). The VA test was also conducted using a computer monitor. Fig. 1 shows some examples of optotype tables.

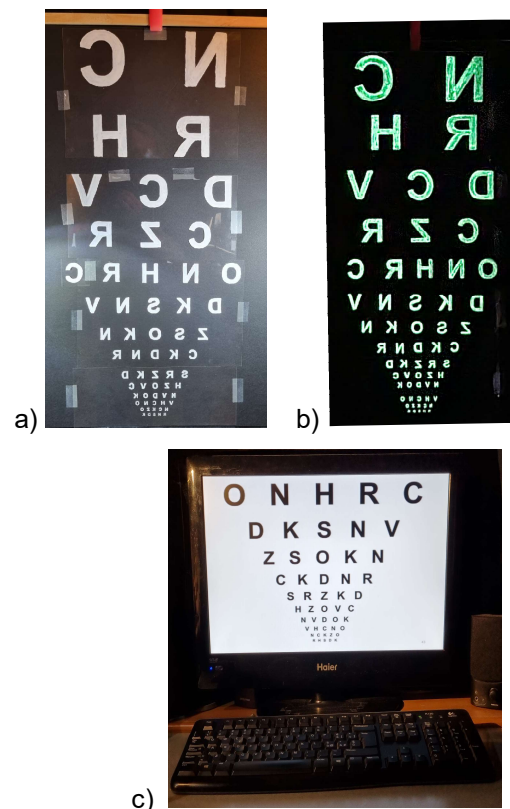


Fig. 2. The LogMAR charts realized in positive contrast on black cardboard, by using white paint (a) and photoluminescent (PL) paint (b). The chart in a) is lightened with white light lamps or with sunlight; the chart in (b) is lightened by UV-A Wood lamps. The characters are inverted because viewed through a mirror. The LogMAR chart is projected in negative contrast by the monitor of a PC (c).

Fig. 2a shows white optotypes drawn on transparent sheets, placed on a black cardboard and lightened by white light lamps or sunlight. Fig. 2b shows PL optotypes drawn on transparent sheets, placed on a black cardboard and lightened by UV-A lamps. Fig. 2c shows an optotypes table projected by a PC monitor in negative contrast. In tests carried out in the dark, the patient is made to observe differently colored cards; If he has truly achieved scotopic vision, he will not distinguish colors because the cones are deactivated. The scotopic vision is reached after about twenty minutes.

B. Luminance measurements

For the test of VA in the light by using the monitor of a PC (see VA test N. 2 in Tab. I), the LogMAR chart is drawn in negative format, i.e., with the bright background and black characters. It is then a matter of measuring the luminance of the background by removing the characters. The measurement of monitor (mo) luminance is simple, because it is homogeneous over the entire surface. To simplify calculations, the monitor was covered with a black cardboard screen (sc) with a hole of known diameter $D=2R=13.7\text{cm}$.

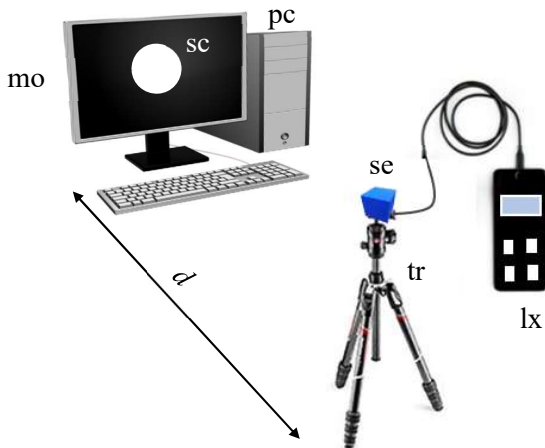


Fig. 3. A schematic experimental set up for measuring the monitor luminance.

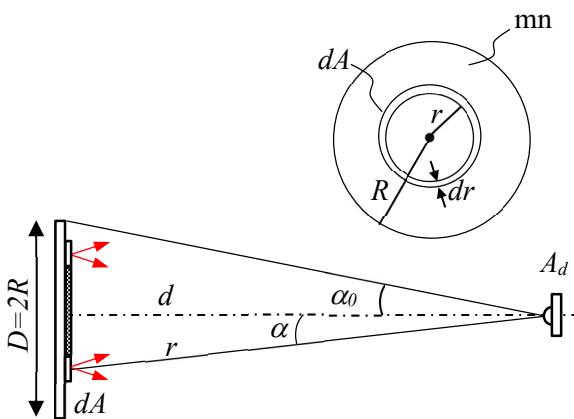


Fig. 4. Schematic of the measure of monitor luminance. The sensor area is $A_d = 363 \text{ mm}^2$.

In front of the monitor, a tripod (tr) was placed on which the sensor head (se) of the luxmeter (lx) is mounted and moved to change the distance d from the screen (see Fig. 3). For measuring the luminance L_v of the monitor, the illuminance E_v is recorded on the luxmeter as a function of the distance (d) between sensor and the monitor. To limit the influence of ambient light, the measurement was carried out in the dark. To understand how to derive luminance from illuminance measurements vs. d , we refer to Fig. 4. As we will see shortly, if the monitor were a Lambertian source and the sensor (se) an ideal absorber, a single measurement of E_v would be enough to derive the luminance L_v , which

is a constant quantity. But this is not the case as already verified in a previous work [3]. We select, on the monitor circle, a portion of area, $dA = 2\pi r \cdot dr$, corresponding to a circular crown, of radius $r < R$, subtending the angle α respect to the sensor center. The elementary luminous flux $d\Phi$, emitted by the elementary area dA , is:

$$d\Phi = \frac{L_v \cdot A_d}{d^2} \cdot \cos\alpha^4 \cdot 2\pi r \cdot dr \quad (1)$$

The total emitted flux, Φ , becomes:

$$\Phi = \frac{2\pi L_v \cdot A_d}{d^2} \cdot \int_0^R dr \cdot r \cdot \cos^4\alpha \quad (2)$$

Moving from variable r to variable α , we have:

$$\begin{aligned} \Phi &= \frac{2\pi L_v \cdot A_d}{d^2} \cdot \int_0^{\alpha_0} d\alpha \cdot \sin\alpha \cdot \cos\alpha = \pi L_v \cdot A_d \cdot \sin^2\alpha_0 = \dots \\ &= \pi L_v \cdot A_d \cdot \{\sin[\text{tg}^{-1}(R/d)]\}^2 \end{aligned} \quad (3)$$

Being the total flux measured by the luxmeter:

$$\Phi = E_v \cdot A_d \quad (4)$$

From Eqs. (3) and (4), we have finally for the luminance of the monitor:

$$L_v = \frac{E_v}{\pi \{\sin[\text{tg}^{-1}(R/d)]\}^2} \quad (5)$$

The experimental data of E_v (lux) give an exponential decay as function of distance d , varied by 6 to 100cm (see Fig. 5).

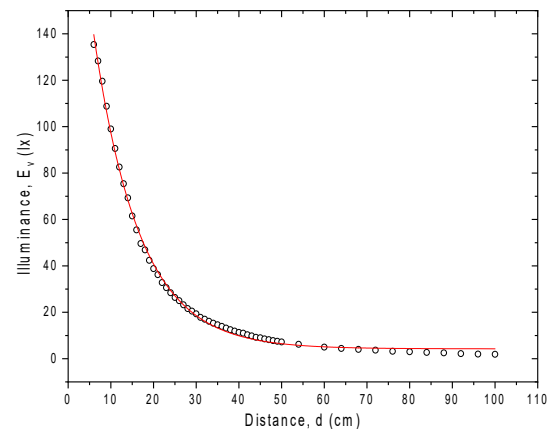


Fig. 5. Results of monitor illuminance as function of distance d , as measured by the luxmeter.

By applying Eq. (5), the monitor luminance shows an exponential growth function with a plateau at high values of d (see Fig. 6). The plateau, of value $L_v = 126.4 \text{ cd/m}^2$, is the average value of luminance when the distance is $> 40\text{cm}$, that is when $\alpha < 10^\circ$. The trend of L_v is explained by considering that the monitor can be approximated to a Lambertian source, that is with constant luminance, only at low angles of incidence on the detector surface, i.e., at distances $>40\text{cm}$ (the experimental condition in which the VA test on monitor was conducted ($d = 2\text{m}$)).

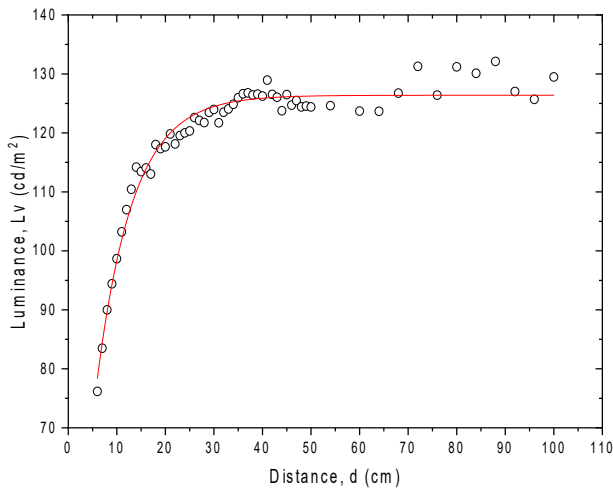


Fig. 6. Results of monitor luminance as function of distance d , as derived from Eq. (5).

For measuring the luminance of decimal chart with black characters in negative contrast (see VA test N. 1 in Tab. I), we have followed the same procedure as above, but keeping the distance above about 35cm. We have designed a circle of white paper sheet (with radius $R = 7\text{cm}$) and illuminated it with a white light lamp (la) (see Fig. 7).

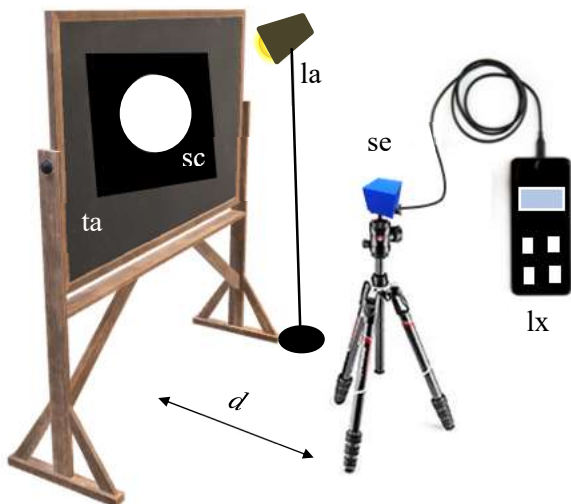


Fig. 7. A schematic experimental set up for measuring the luminance of a decimal chart. The lamp (la) is a white light source.

Due to the presence of a strong background of light from the lamp, we had to make two sets of measurements. In the first one, the white circle was illuminated, thus measuring the illuminance due to the white circle and the ambient light; in the second one, we have darkened the circle with a black cardboard, measuring in this way only the illuminance due to the environment light. Subtracting the two results, we finally obtained the illuminance due to only the white source.

The illuminance curve of the disk source, as a function of distance, shows, as for the measurements on the monitor, an exponential decay (see Fig. 8).

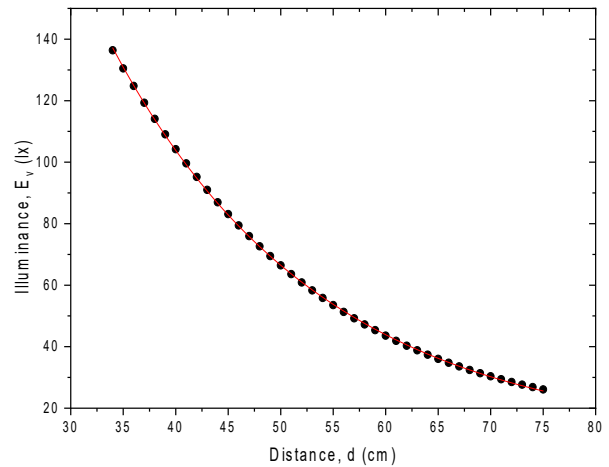


Fig. 8. Result of the illuminance measured by the luxmeter, as function of distance d from the illuminated disk source.

From the curve of the E_v due to the source alone, we derive the curve of the source luminance, L_v , which we expect to be constant. And, in fact, the curve is rather flat with an average value of $1055 \pm 56 \text{ cd/m}^2$.

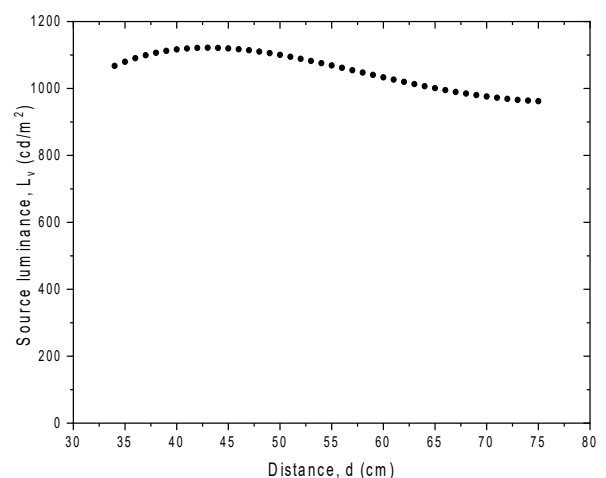


Fig. 9. Result of luminance of the white disk of Fig. 7, as function of distance d , as derived from Eq. (5).

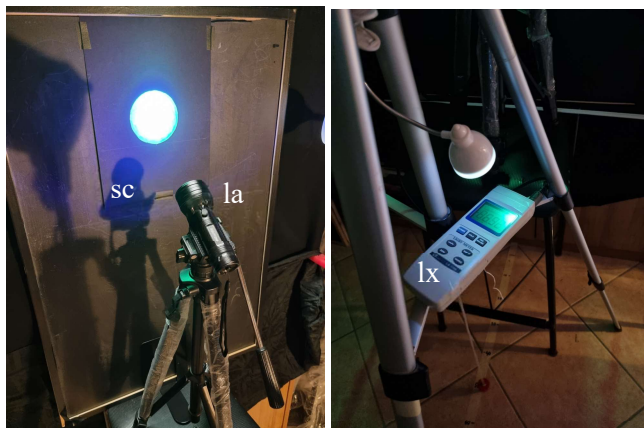
The measurement of luminance L_v of a source obtained by reflecting light on a surface, as is the case of the white surface illuminated by lamps in Fig. 7, can be obtained in an alternative way. Approximating the surface source to a Lambertian source, its luminance can be expressed by the simple formula [4]:

$$L_v = \frac{E_s \cdot R_s}{\pi} \quad (6)$$

where E_s is the illuminance produced by the lamps on the source surface and R_s is the average reflectance to white light of the surface itself. Therefore, by measuring E_s and calculating L_v , we can derive the reflectance of

the surface by Eq. (6). A series of 24 measurements of E_s , distributed over the entire surface of the circular source of Fig. 7, gave the following mean value: $E_s = 3818 \pm 152 \text{ lm/m}^2$, which, combined with the mean value of $L_v = 1055 \pm 56 \text{ cd/m}^2$, gives for the mean reflectance of the white paper sheet: $R = 87 \pm 8\%$. This value is very realistic for a white cardboard surface [5]. The knowledge of R allows us to obtain the luminance of a light reflecting source from illuminance measurements on its surface, through Eq. (6). Eq. (6) cannot be used, of course, to measure the luminance of a monitor (Fig. 3) or of a PL source.

For measuring the luminance of the PL characters of a LogMAR Chart used in the dark, I adopted the same scheme shown in Fig. 7. The circular target is now obtained by passing three coats of yellow/green PL paint on the transparent sheet masked by the black cardboard. The target is then illuminated with Wood's lamp (la) at $\lambda=395\text{nm}$ fixed on a tripod 20cm away and inclined of 45° (see photo in Fig. 10a).



a) b) c)

Fig. 10. Photos of the apparatus for measuring the luminance of the LogMAR chart PL characters in dark conditions. a) Illumination of the circular PL target by the Wood lamp; b) the illuminance value on the luxmeter is read in the dark by using a small LED lamp; c) the sensor of the luxmeter is mounted on the tripod.

The luminescence light decays very quickly, with a measured time constant of $\tau=1.4 \pm 0.1 \text{ s}$, so, during the measurements, the lamp was kept lit and pointed at the target. The measure of E_v as a function of distance d was made with the luxmeter (lx) placed on a second tripod (see the photos in Figs. 10b and 10c). Applying the Eq. (5), a luminance of $L_v = 190 \pm 10 \text{ nit}$ was finally found. The measurement of the luminance of the white characters of a LogMAR chart (see Fig. 2a), exposed to sunlight, was obtained by measuring the irradiance E_s on the surface and applying Eq. (6), placing $R_s \sim 0.9$.

III. INTRODUCTION TO THE TEST METHODS

A. Morphoscopic Acuity

The visual acuity of recognition, or morphoscopic acuity, is defined by the minimum angular dimensions necessary to allow the recognition of certain symbols [6-15]. The capital letters of the alphabet are the most widespread and used for their ease of use. There are various modes of expression of visual acuity: (i) the Snellen scale of 20 feet; (ii) the Snellen scale of 6 meters; (iii) the Monoyer decimal scale; (iv) the LogMAR scale, where MAR is the minimum angle of resolution, that is the angular size of the critical detail that must be resolved by the patient to identify the optotype correctly. Fig. 11 shows the schematic of a morphoscopic acuity test. The use of a mirror in the optical path allows to double the physical distance between the subject and the chart. Of course, since the mirror rotates the letters 180° around the vertical axis, the optotypes on the table were also drawn rotated of 180° .

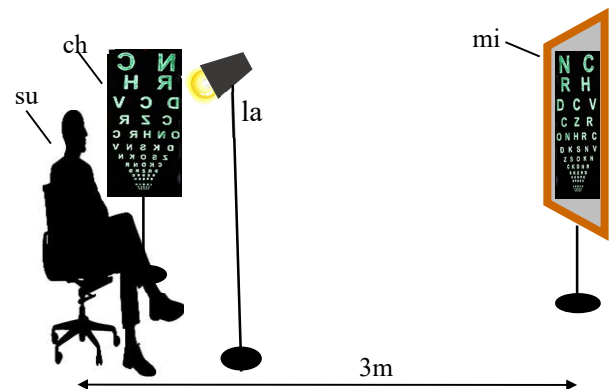


Fig. 11. Test of visual acuity (VA) carried out doubling the optical path to $d = 6\text{m}$ by using a mirror (mi). (su) subject; (ch) chart; (la) lamp. For the test at dark, the PL characters are lightened by a UV-A lamp (la).

In Tab. I, the different types of tests performed to evaluate the visual acuity (VA) of a subject using Monoyer decimal or geometrical (LogMAR) charts, are summarized, considering: i) the environment (Env), whether illuminated (L) or dark (D); ii) the type of illumination of the chart (Illum), by a lamp light, a monitor, the Sun or UV-A; iii) the type of chart (Chart), if Monoyer decimal (Dec) or LogMAR (LM); iv) the optical distance between chart and subject (d in meters); v) the background (BG) of the chart, if white paper (WP), white screen (WS) or black paper (BP); vi) the character (Char), whether black, or white, or PL.

TABLE I. SUMMARY OF AV TESTS CONDITIONS

N	Env	Illum	Chart	d (m)	BG	Char
1	L	Lamp	Dec	3	WP	Black
2	L	Mon	Dec	2	WS	Black
3	L	Sun	LM	6	BP	White
4	D	UV-A (395nm)	LM	6	BP	PL
5	D	UV-A (365nm)	LM	6	BP	PL

The types of tests performed to assess a subject's visual acuity (VA) by using decimal or LogMAR charts.

The LogMAR chart, used in the light or in the dark, uses white or luminescent characters (positive contrast), respectively, and was drawn for a distance $d = 6m$ (see Table I), whereas the decimal chart was used at light with black characters (negative contrast) and was drawn for a distance $d = 2m$ and $d = 3m$ (see Table I). The tests in the dark were done by illuminating PL characters in two ways: i) with Wood's lamp at $\lambda=395nm$; ii) with Wood's lamp at $\lambda=365nm$, as indicated in Tab. I.

Visual acuity is nowadays scored with reference to the logarithm of the minimum angle of resolution, MAR, expressed in prime degrees [8, 12, 15]. The Bailey-Lovie LogMAR test chart with 14 lines of optotypes is shown in Fig. 13. The range of dimension of L is 20 times (see Table II), and then, to better distinguish the characters in the figure representing the chart, this was divided into two parts, the first one from line 1 to 7, and the second one, of double size, from line 8 to 14. The quantity LogMAR is equal to $\log_{10} MAR (')$. As it can be seen, the progression of characters dimension is linear with LogMAR. The other advantage of the LogMAR chart is that it contains only five characters per line, and this makes the assigned VA value more precise. In our case, we have simplified the chart reducing the number of characters on the first four lines, so as not to have to deal with excessive horizontal dimension of the chart itself. The Bailey-Lovie chart uses rectangular (5:4) alphabetic characters. Fig. 14 shows the optotype E, generally taken as an example for illustrating the relationship between the angle MAR , L , the height of character, and $P=L/5$, the limb of letter E representing the minimum distinguishable particular from which the angle MAR is derived. The values of visual acuity, expressed in Monoyer tenths, x , are given in Tab. II together with angle MAR , expressed in prime degrees, and the height of the character, L , expressed in mm, given by:

$$L = d \cdot \frac{10}{x} \cdot 0.29 \cdot 5 = 1.45 \cdot d \cdot \frac{10}{x} = 1.45 \cdot d / VA \quad (7)$$

where d is the distance in meters, $10/x = MAR(')$, $0.29=1000 \cdot \text{tg}(1')$, and $x/10$ is the decimal VA.

Old charts are of type Monoyer decimal. Fig. 12 shows the decimal optometric table, calculated for a distance $d=3m$. On the left column is reported the height L of characters, in mm, whereas on the right column is reported the visual acuity VA expressed in tenths $x/10=d/L$. One of the drawbacks of the Monoyer decimal scale, as well as the Snellen scale, is that the font sizes of lines with lower visual acuity change more markedly than those of high visual acuities. This prevents a good distinction between high visual acuities. The other drawback is that the number of characters is not constant in the different lines.

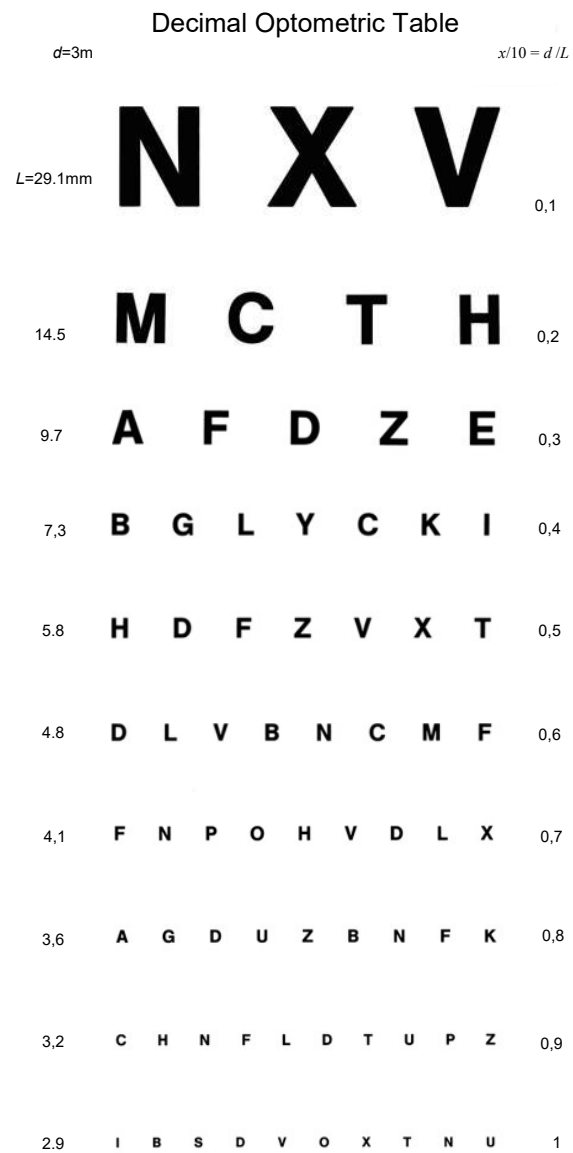


Fig. 12. The Decimal Optometric Table with 10 lines of optotypes. On the left column is the height L of characters; on the right column is the VA expressed as $x/10=d/L$, where d is the distance expressed in meters and L is expressed in mm.

TABLE II. VISUAL ACUITY CONVERSION TABLE.

n line	x VA (tenths)	L (mm) d=3m	L (mm) d=6m	MAR (')	Log MAR VA
1	1	43.6	87.3	10	1.0
2	1.3	34.6	69.3	7.94	0.9
3	1.6	27.5	55.1	6.31	0.8
4	2	21.8	43.7	5.01	0.7
5	2.5	17.3	34.7	3.98	0.6
6	3.2	13.8	27.6	3.16	0.5
7	4	11.0	21.9	2.51	0.4
8	5	8.7	17.4	1.99	0.3
9	6.3	6.9	13.8	1.58	0.2
10	7.9	5.5	11	1.26	0.1
11	10	4.4	8.7	1	0.0
12	12.6	3.4	6.9	0.79	-0.1
13	15.9	2.7	5.5	0.63	-0.2
14	20	2.2	4.4	0.5	-0.3

This table shows how the quantities MAR (the Minimum Resolution Angle expressed in primes), L (height of the character, calculated for 6m and 3m distance) and x (the visus expressed in tenths= $10/MAR$) vary as a function of LogMAR (the decimal logarithm of the Minimum Resolution Angle) with steps of 0.1 from 1.0 to -0.3.

This affects the way to give a value to visual acuity, as we will shortly see. Despite this, some preliminary tests have been done by us at light with this table, as specified in Tab. I.

Visual acuity in tenths, x, varies from a minimum of 1 for the largest characters in the first line, to 10 for the smallest characters. As it can be seen, the decimal scale in Fig. 12, with arithmetic progression, is traced linear with respect to the tenths of VA, whereas the LogMAR scale in Fig. 13, with geometric progression, is traced linear with respect to the logarithm of the MAR. The curiosity of this terminology is that, although the decimal scale is arithmetic, the font size does not vary linearly, while it varies linearly in the LogMAR scale.

The recording of visual acuity using the decimal chart follows this criterion: x VA = x value of the best line read, followed by a number of plus (+) signs of characters read in the following line, ignoring the results on the other lines below. If the patient is unable to read

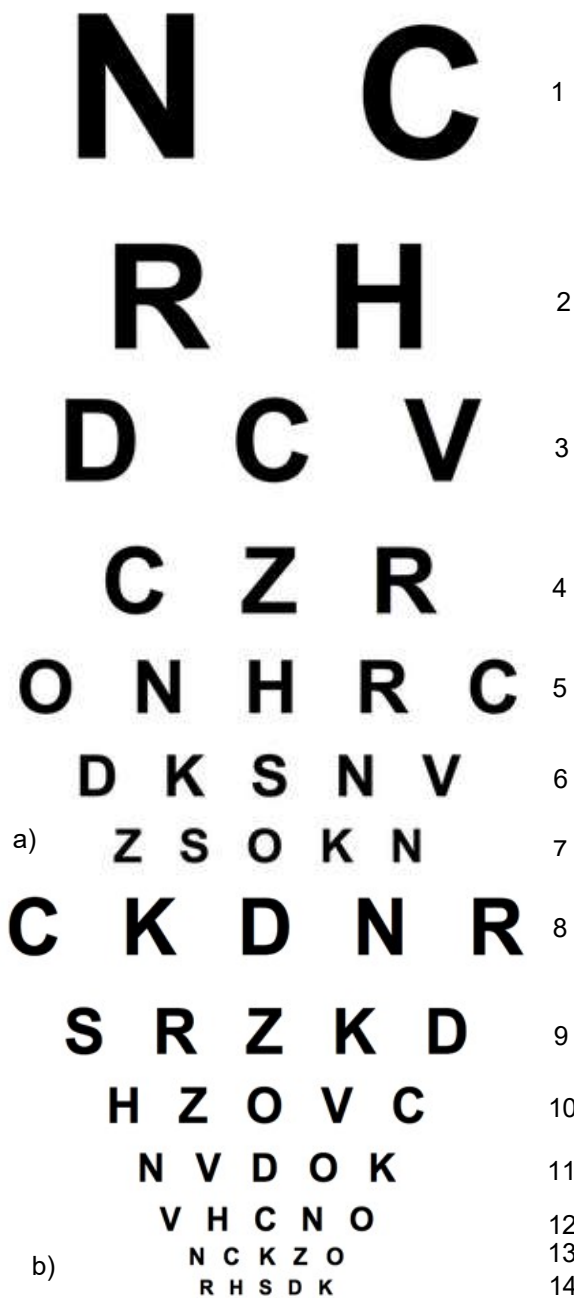


Fig. 13. The Bailey-Lovie LogMAR test chart with 14 lines of optotypes. The font size in b) (the first 7 lines) is doubled compared to a) (the second 7 lines). On the right is the line number.

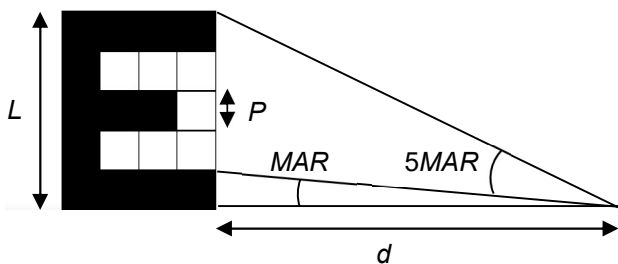


Fig. 14. The letter E, taken as an example, allows to show the relationship between the quantities L, P, MAR and d.

all of the letters on a particular line, it is a standard practice to assign a VA to the smallest line for which the patient is able to read at least half the letters. Any errors are indicated by a minus superscript, while additional letters identified correctly on the subsequent line are shown with a plus superscript. From here we understand that in the Snellen and Monoyer decimal system, where the number of characters per line is variable, the criterion for assigning a line as read, is not consistent with the different lines, while it is for the LogMAR system, in which the number of characters per line is constant and equal to five (apart our arbitrary choice of reducing the number of characters in the first four lines, as shown in Fig. 13). The recording of visual acuity using the LogMAR chart follows this criterion [6]: the total score for a line on the LogMAR chart represents a change of 0.1 log units [9]; The score decreases as visual acuity improves. If a line contains five letters, each letter has a score value of 0.02 log units. The formula used in calculating the score is therefore:

$$\text{LogMAR VA} = \text{LogMAR of the best line read} - 0.02 \times X \quad (8)$$

where X is the number of letters read correctly in the line below. Following Rosenfield and Logan [10], X is the number of letters read correctly in the lines below, irrespective of their position on the chart.

A further method of scoring the VA is the VAR (Visual Acuity Rating) of Bailey, which consists of multiplying the tenths of the best line read by 10 and adding or subtracting units for each wrong or right character, respectively. Example: Subject reads all letters of x/10=10/10: VAR score =100. If one letter is wrong, VAR=99; if two letters are wrong, VAR=98. If instead he reads a letter after 10/10, then VAR = 101.

B. Tests in an external photometric laboratory

The tests presented above were accompanied, for comparison, by those carried out in an external optometric laboratory. The purpose is twofold, that is, to validate the results of the common tests, and to have a more complete picture of the patient's vision acuity, considering that our tests can be slightly different from those required by the optometric protocol. The visual tests were carried out on two patients: A (the corresponding author, adult) and B (the coauthor, young). External laboratory tests refer to both far (F) and near (N) distance vision; however, our attention will be limited to the visus for the far. Tabs IIIa, b are the protocol tables. They are generally accompanied by two graduated lunettes reporting the angular information (from 0° to 180°) on astigmatism, as will be explained later (see Fig. 15). The symbols on Table III are the following:

- D: Distance, if far (F) or near (N).
- OD: Oculus Dexter (right eye).
- OS: Oculus Sinister (left eye).
- OU: Oculus Uterque (both eyes).
- SPH: Sphere; stands for the power of the lens that will correct the eyesight.

CYL: Cylinder; stands for the amount of astigmatism in the eye. The cylinder and axis appear always together and are used to correct the astigmatism.

AX: Axis; is a degree between 0° and 180°, and indicates exactly where the astigmatism appears on the eye.

ID: interpupillary distance.

TABO or INT (International): refer to the system used for calculating the axis of the left eye.

TABLE III. FACSIMILE OF THE TABLES USED IN THE PHOTOMETRIC LABORATORY.

	OD			OS		
D	SPH	CYL	AX	SPH	CYL	AX
F						
N						

a)

Interpupillary distance			Visus		
OD	PD	OS	OD	OU	OS

b)

Tables to be filled with the visual acuity data.

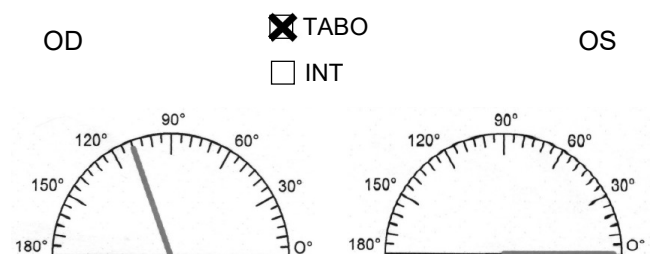


Fig. 15. The two lunettes representing the angular orientation system used to indicate the degree of astigmatism, for OD and OS, respectively.

Now let's see how to interpret the information reported in Table III. Let's consider either of the two eyes. The minus sign in the SPH box indicates that the subject is nearsighted, whereas the plus sign in the SPH box indicates that the subject is farsighted. If the SPH box is empty, then the subject is emmetrope, that is, he has no visual defects. The absolute value of SPH indicates the gradation of the lens necessary to correct the defect: the higher it is, the greater the defect. Eyeglass strength is measured in diopters. If the prescription reads -0.25, that means the eyeglasses need 0.25 diopters of strength to correct nearsightedness.

Nearsightedness, or myopia, is a common refractive disorder. If the subject is nearsighted, he can see objects that are close clearly, but objects that are

farther away will look blurry. With nearsightedness, the eye is usually elongated, with too much distance between the cornea at the front and the retina at the back. Nearsightedness can also happen if the cornea of the eye is too curved. Due to this increased distance, light rays fall in front of the retina, instead of on it. This can cause the distance vision to be fuzzy. For a nearsighted prescription, the strength of the lenses is marked with a minus sign.

Farsightedness, or hyperopia, is a refractive disorder that makes close objects harder to see than distant objects. It happens because the distance from the cornea to the retina is too short or because the cornea of the eye is not curved enough. If the subject is farsighted, light focuses behind the retina instead of squarely on it. For a farsighted prescription, the strength of the lenses is marked with a plus sign.

Now let's move on to the box marked CYL: if there is any value it means that the subject is astigmatic. This visual defect is given by a different sphericity of the cornea, which implies a different angle of the axis. The CYL section must always be filled in together with the axis field. The astigmatism is of myopic type if the values of SPH and CYL are both negative, while it is of hypermetropic type if the values of SPH and CYL are both positive. If the signs in the SPH and CYL boxes are different, we are in the presence of a mixed astigmatism. If the CYL box contains a digit, then there will also be a value for AX. AX indicates the obliquity of the meridian deviated by astigmatism. Generally, this is given by a slightly elongated cornea, whose correction requires the use of special lenses, called toric. This value can range from 0° to 180° and indicates the orientation that the corrective lens must have. The degrees required for the correction of astigmatism can be indicated graphically by semicircles, relating to the individual eyes.

Astigmatism is an irregular curve in either the crystalline lens or the cornea of the eye. This irregular curve can bend the light that enters the eye and affect the way it hits the retina. Astigmatism can blur both near and far objects. It can also distort the images. If the astigmatism measures 1.5 diopters or more, the subject may need to wear prescription glasses or contact lenses to see properly.

The difference between TABO and INT lies in the direction of indication of the axis: in TABO, the axes of both eyes are indicated counterclockwise; in INT, the left eye is measured clockwise, while the right eye is measured counterclockwise. TABO is the universal system. If AX values are indicated with the INT system, to obtain the angle of the left eye in TABO it is necessary to subtract the INT value from 180:

$$\text{Axis TABO} = 180 - \text{Axis INT} \quad (9)$$

Interpupillary distance (or ID) is the distance between the pupils when looking forward. It is a necessary measure to be able to position the optical center of the lens directly in front of the pupils. It is measured in millimeters and the optimal value is between 54 and 74 mm; the average pupillary distance in Italy is 62 mm.

C. Test of the Angle of View in the Dark

This test highlights the disappearance of particular light sources in the dark when they are confined within the dark cone projected from the inner part of the fovea (foveola). We will investigate this phenomenon using a circular PL sticker (PL target) as test field and measuring, in the dark, the distance at which it disappears from view. Of course, the darkening of the PL target takes place only when its luminance is very low (but impossible to measure by us), a necessary condition in order not to activate the photoreceptor cones.

This test, "test of the angle of view in the dark", is intrinsically linked to the condition of darkness, and therefore has no equivalent to those carried out in the light. To well understand this phenomenon, let's review a simple optical model of human eye (see Fig. 16) [7].

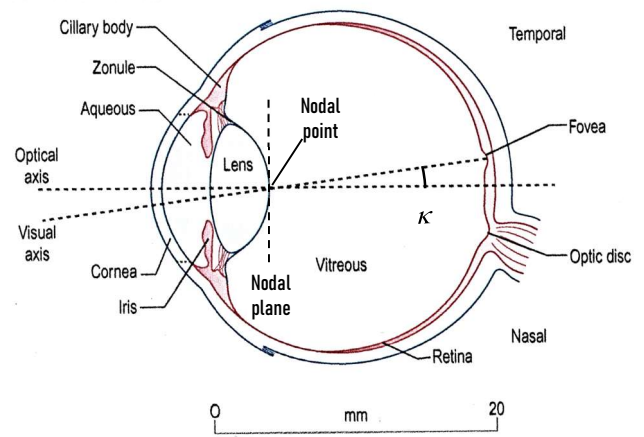


Fig. 16. This simple model of the human eye shows the main elements that underlie vision.

The human eye is composed of two positive lenses, the cornea and the crystalline lens, that project images of the world onto the retina. The eye of an adult human has a longitudinal axial length (LAL) of about 24-25mm, and the group made of cornea, plus aqueous humor, plus crystalline lens extends for about a third of this length. The iris is the vascular membrane of the eye, pigmented and with the shape and function of diaphragm, located behind the cornea and in front of the crystalline lens, perforated by the pupil, the hole of the eye in the center of the iris. The pupil, depending of ambient light, has a diameter from 2mm in bright light to 8mm in the dark.

The light, refracted by the cornea (a lens with a fixed optical power and refraction index $n = 1.376$) and the crystalline lens (an active element able to modify its optical power and refraction index $n = 1.375 \div 1.406$), crosses the vitreous humor and reaches the central area of the retina, the fovea, where photoreceptors specialized for vision in the light (cones) are densely packed and provide an image with the highest resolution. The peripheral part of the retina renders lower resolution, but specializes in movement and

object detection in the visual field. It contains photoreceptors (rods) specialized for vision in the dark.

We distinguish two axes for the eye: the optical axis, perpendicular to the cornea and intersecting the center of the entrance pupil, and the visual axis, connecting the fixation point in the object space to the nodal point and to the fovea (see Fig. 16). The angular distance between these axes is the angle kappa (κ) [9], which, for an average eye is around 4° horizontally in the temporal direction and 0° vertically.

Now let's examine the retinal image and calculate the corresponding angle of view. Fig. 17a shows a section of the retina where ganglion and bipolar cells, rods and cones are highlighted. The image on the retina is formed at the fovea, which is a concave area rich in cones (see Fig. 17b). The central area of the fovea, foveola, has only cones of very small diameter and with a high density (~147,000 / mm²). On the foveola (fovea centralis) the image of an object is formed with the highest resolution. The visual acuity (VA) is the highest in the fovea and undergoes a sudden reduction outside it. The size of the retinal image, h , is related to the distance between the retinal plane and the mean nodal point (about 17mm), s , and to the angle of view, α , from the relation:

$$h = \text{tg}\alpha \cdot s = \text{tg}\alpha / \mathcal{D} \quad (10)$$

where \mathcal{D} is the optical power of the eye, expressed in diopters (1 diopter = 1m⁻¹).

The total optical power of the relaxed eye in humans is then approximately 60 diopters, of which, the cornea accounts for approximately 40 diopters and the crystalline lens for the remaining 20 diopters (from 17 to 22). For a retinal image size of 0.3-0.4mm, the angle of view, α , becomes around 1°-1.3°, respectively.

Fig. 17a shows the internal structure of the wall of the eye and the detail of a portion of the retina near the fovea, with the different types of cells and photoreceptors. At the fovea, the thickness of the retina is reduced forming a concavity, because the layers of ganglion and bipolar cells are bent towards the periphery (see Fig. 17b).

This part is dedicated to measuring the angle of view, α , in dark conditions. Being that the cones are deactivated in the dark, the consequence is that the area of the fovea is depleted of active photoreceptors, and, in particular, the entire area of the foveola, rich only in cones, becomes practically blind, while instead the rods remain active in the entire retina. The direct view of an object will then be prevented if the angular extension of its image on the foveola is smaller than the angle of view. When the cones of the foveola are deactivated, the sight of a source with low luminance is made possible by the cones placed on the edges of the fovea.

To measure the angle of view in the dark the test is organized in the following way. On a wall with a dark background, a photoluminescent circular sticker (a PL target), of yellow or light green color and of about 1cm in diameter, is fixed at the level of the eyes of the subject (see Fig. 18). He will remain in the dark for 15-20 min to

make sure the cones are deactivated [1, 2]. During the measurements, the sticker can be illuminated with a Wood's or a white light lamp, but a Wood's lamp is more effective.

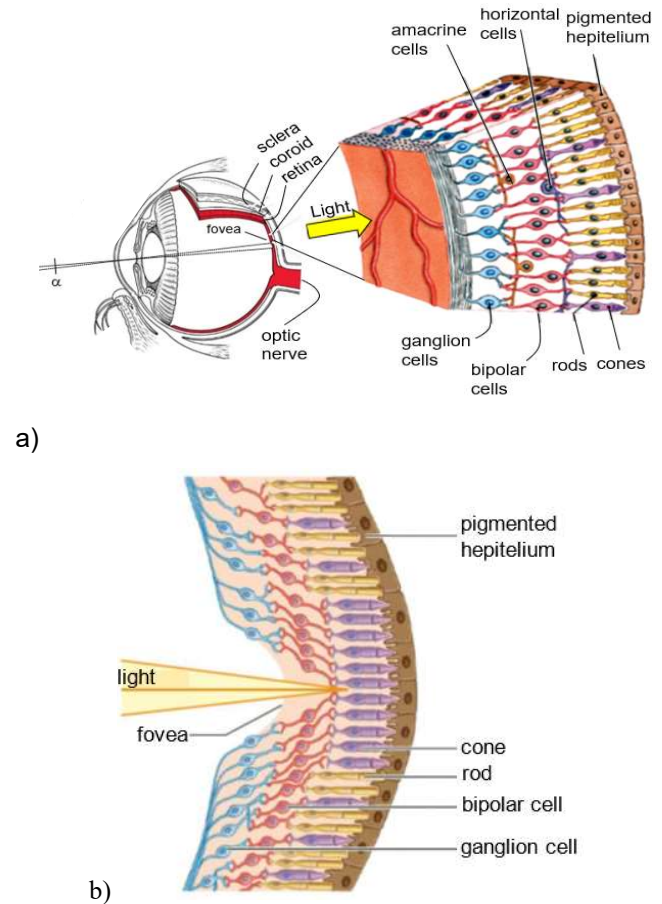


Fig. 17. The model of the eye in the figure shows the composition of the back wall of the eye and the layers of cells forming the retina.

To this end, to avoid reactivating the cones, the subject will take care to keep his eyes tightly closed during this operation. The luminance of the sticker must be very low for conducting an effective test, but its intensity is unknown because impossible to be measured by us. The test was carried out both on the individual eyes, dressing shielded glasses or a hood with hole for the testing eye, and on both ones. The subject will then start from a distance of about 20 cm from the wall observing the sticker and moving away from it gradually noting the distance with a laser pointer, and avoiding turning on the light during the distance measurement. The measurement of distance with the laser device must be made by approaching the device on the cornea of the eye under test. To this end, it would be useful to carry out the test in presence of another person who will take care of measuring the distance in the dark.

Moving away from the sticker, the subject will notice that, at a certain distance, the PL target will tend to disappear and that it will disappear completely moving further away. At that point the subject will make distance measurements at smaller intervals, approaching and

moving away from the target, in order to identify precisely a distance, $d = d_{min}$, at which the sticker appears dark (see Fig. 18). By measuring the distance d_{min} and the PL sticker diameter D , the angle of view will be easily determined.

In conclusion, this test allows to determine the angle of view, α , that is one of the three variables of Eq. (10). By knowing one of the other two variables, h or s , we would know the geometry of eye in terms of distance between the retinal plane and the mean nodal point, s , or of extension of the foveola area, h , respectively.

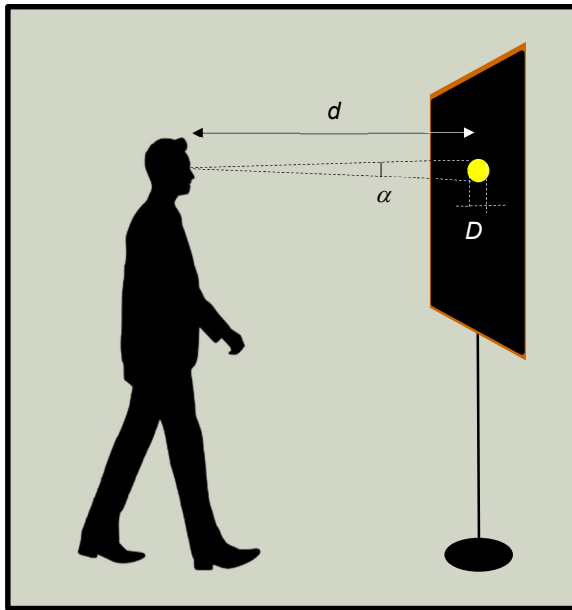


Fig. 18. The subject is shown fixing his gaze, in the dark, on the PL sticker at distance d . When, moving away from the sticker, this will disappear, then it will subtend an angle equal to the angle of view α .

The distance measurements, d , were made using the digital laser distance meter, and a single Becho PL target, of diameter $D=19.7\pm 0.3\text{mm}$, illuminated with Wood lamp, at $\lambda = 395 \text{ nm}$. The measurement of the distance between observer and target is made by approaching the back of laser box to the cornea of the eye and pointing the laser beam to a point near the target. The correct distance to apply is obtained by increasing the measured distance of $\sim 7\text{mm}$, the distance from the nodal point of the eye (see Fig. 16) to the target [2]. This small correction, however, does not change significantly the result of α .

Referring to Fig. 18, we have the following angle of view, and its error, in correspondence to d_{min} :

$$\alpha = 2 \cdot \text{tg}^{-1} \left(\frac{D}{2 \cdot d_{min}} \right) \quad (11)$$

$$\Delta\alpha = \left(\frac{4}{4d_{min}^2 + D^2} \right) \cdot (D \cdot \Delta d_{min} + d_{min} \cdot \Delta D) \quad (12)$$

D. The Blind Spot Test of Mariotte

The blind spot in the visual field of a human eye was discovered in 1668 by the French scientist Edme Mariotte (1620–1684), member of the Académie Royale des Sciences in Paris and famous for his experiments on vacuum that led to the famous law of Boyle and Mariotte [16-20].

Today, this phenomenon is also known as the Mariotte's spot in visual field. In a letter written to Pecquet in 1668, he announces the discovery of the blind spot, specifying his observation of the lack of vision which occurs when an image of an object falls solely on the optic nerve. In addition, Mariotte explains that the anatomy of a man reveals that the optic nerve, the optic papilla devoid of photoreceptors, is never located exactly in the middle of the fundus of the eye and that it is a bit higher, and on the nose side.

Fig. 19 shows a horizontal section of the human eye, in which the cornea (1), the aqueous humor (2) and the crystalline lens (3) are highlighted on the front. On the back are highlighted: the retina (4), the choroid (5), the sclera (6), the fovea (7) with its characteristic depression profile, the optic nerve (9) at the base of the papillary disc (8) and finally the venous (10) and arterial (11) blood vessels, which depart together with the optic nerve. This schematic representation of the human eye corresponds to what anticipated by Mariotte's works.

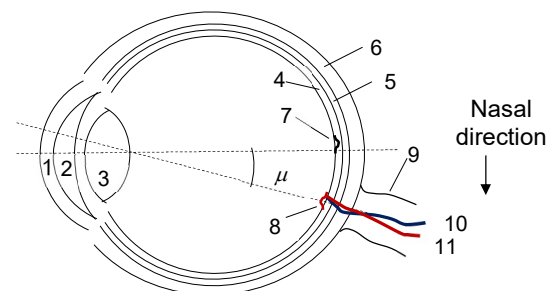


Fig. 19. Horizontal section of the eyeball of the right eye, in which the location of the papilla (8) of the optic nerve is highlighted, which is the subject of this section.

The eye represented in Fig. 19 is the right one, in which, as we see, the papilla of the optic nerve is shifted downwards, that is, towards the nose in the horizontal direction. By symmetry, the same representation for the left eye would see the papilla shifted upwards, that is, still towards the nose.

We have already seen in the previous section how the fovea is displaced, with respect to the optical axis, by about 4° . In the case of the papilla, the misalignment with respect to the optical axis, which we call angle μ in honor of Mariotte, is around 15° on the nasal direction (see Fig. 19), and around 2° vertically up. The papilla is of about 2mm size, corresponding to 7° vertically and 6° horizontally. The papilla is blind, that is, devoid of photoreceptors, it therefore appears as a blind spot in the visual field (physiological scotoma or Mariotte's spot), but its presence is not felt by normal sight, because the mind implements a filling (papillary filling)

of the missing visual field. Moreover, in binocular vision, only one papilla is blind respect to a fixed direction, due to the symmetry of the eyes with respect to the nasal axis.

However, there is a simple method to highlight the presence of the Mariotte stain (blind spot test of Mariotte), and consists in fixing on a wall two small stickers at a horizontal distance H , standing in front of the left one, fixing it with the right eye and covering the left eye at the same time (see Fig. 20a). Moving away from the wall for a variable distance d , about three times H , the observer will notice that the right sticker no longer appears in the field of view.

The angle of the horizontal misalignment of the papilla, with respect to the optical axis, will then be given by $\tan^{-1}(H/d)$, and of the order of 15° . Fig. 20a shows an outline of the Mariotte test. Of course, the test must also be done on the left eye by reversing the terms left / right.

In this way we will have found the horizontal misalignment of the papilla for the two eyes. The experiments have been performed both in the light, using two black stickers on a white wall, and in the dark using two photoluminescent stickers on a black wall.

In Fig. 20a the subject is shown in front of the wall with the two stickers. Fig. 20b shows schematically the pattern of the two eyes from above on a transversal plane, with the right eye pointing at sticker (2) and the left eye blindfolded.

The light emitted by sticker (2) reaches the fovea and is directly seen, whereas the light emitted by sticker (1) reaches the right eye at an angle μ and hits the blind papilla; as a consequence, the sticker (1) is not seen. The OS eye must be blindfolded because, otherwise, the target 1 would appear on that part of the retina free of the papilla.

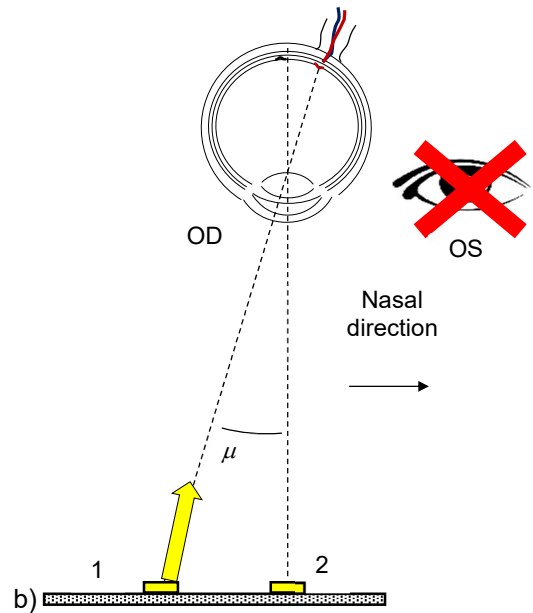


Fig. 20. Schematic representation of the Mariotte's blind spot test. The observer is in front of two PL stickers in the dark (a). Scheme of the two eyes and the two stickers seen from above (b). The image of sticker 1 fall on the papilla and then disappears.

Mariotte's blind spot test does not involve a single μ measurement, as simplified in Fig. 20, but an interval one on the horizontal plane, as illustrated in Fig. 21 [17]. In fact, at varying the distance of the subject from the target, there is a significant interval between the minimum distance d_{min} at which the target disappears and the maximum distance d_{max} at which it reappears. These two distances correspond, respectively, to the angles, μ_{max} and μ_{min} , which limit the angular range of invisibility of the papilla.

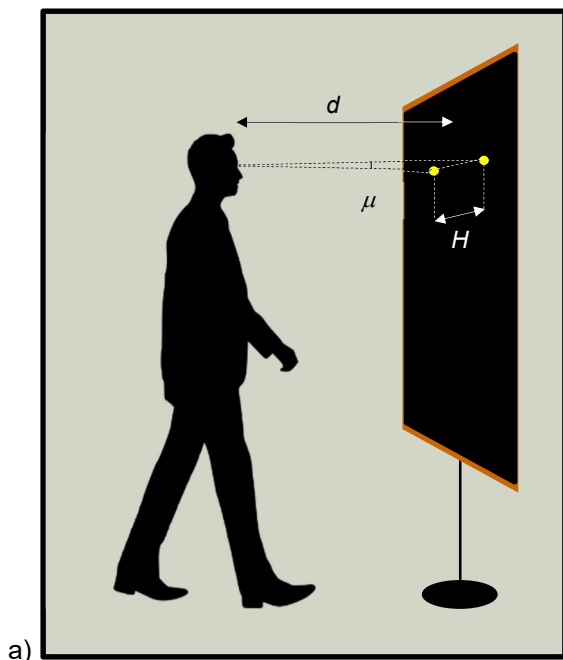
Fig. 21 shows the geometry of the test. On the right the detail shows the two lines, inclined with respect to the visual axis, that define the angular limits, for an indirect view, within which there is no visibility, because the image of the object falls on the papilla. Referring to Fig. 21, we have the following expressions for μ_{max} and μ_{min} , and their errors, in correspondence to d_{min} and d_{max} :

$$\mu_{max} = \operatorname{tg}^{-1}\left(\frac{D}{d_{min}}\right) \quad (13)$$

$$\Delta\mu_{max} = \left(\frac{1}{D^2 + d_{min}^2}\right) \cdot (D \cdot \Delta d_{min} + d_{min} \cdot \Delta D) \quad (14)$$

$$\mu_{min} = \operatorname{tg}^{-1}\left(\frac{D}{d_{max}}\right) \quad (15)$$

$$\Delta\mu_{min} = \left(\frac{1}{D^2 + d_{max}^2}\right) \cdot (D \cdot \Delta d_{max} + d_{max} \cdot \Delta D) \quad (16)$$



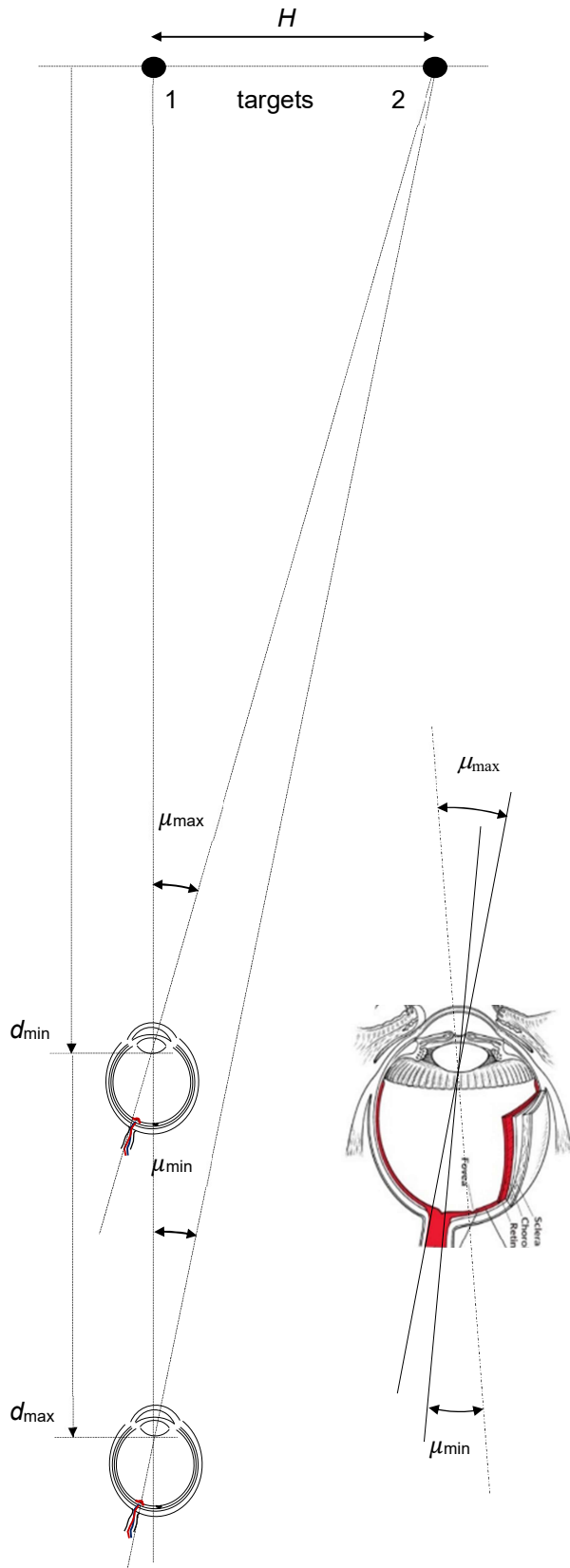


Fig. 21. The figure shows the origin of the angles μ_{max} and μ_{min} , associated, respectively, with the distances d_{min} and d_{max} , at which the target 2 disappears, or reappears, respectively, when the distance d of the eye from target 1 is increased.

E. The Combined Test of the Angle of View in the Dark and the Mariotte's Blind Spot Test

The test of angle of view and the Mariotte's blind spot test can be combined in the dark (see Fig. 22). This test must be prepared as if Mariotte's test was performed in the dark. The dark condition is necessary in this case to repeat the angle of view test (see Fig. 18). To combine the two tests, that is to have both targets disappeared, this is the procedure to follow: i) fix a value for $H=H_0$; ii) from H_0 find $\mu_{0,max}$ from the μ vs. H function (see the results section); iii) from H_0 and $\mu_{0,max}$ derive $d_{0,min}$ (see Fig. 22); iv) apply the following equation to find D_0 , the targets diameter:

$$D_0 = 2 \cdot d_{0,min} \cdot tg(\alpha/2) \tag{17}$$

Under these conditions, target 1 will not be visible in the range $d = d_{min} \div d_{max}$, while target 2 will not be visible at $d \geq d_{min}$.

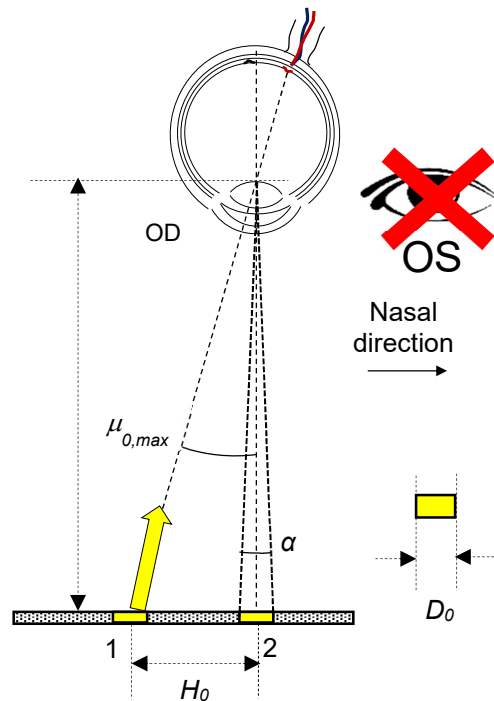


Fig. 22. Schematic representation of the Mariotte's blind spot test combined with the angle of view test in the dark. The observer doesn't see target 1 because of the effect of Mariotte's angle μ , and doesn't see target 2 because, in the dark, this falls within the angle of view α .

F. Test of Resolution Acuity or of the Minimum Angle of Resolution

The smallest resolvable angle expresses the smallest distance between two lines so that they are perceived as two separate objects. The solvable minimum has values greater than the visible minimum. Theoretically, to detect distinct two lines it is necessary the activation of two photoreceptors and between them the presence of a deactivated photoreceptor that indicates the lack of continuity. In the normal eye (emmetrope) the resolution acuity is about 35-50 arcseconds. Specific symbols such as Landolt's "C" can

be used to quantify this type of visual acuity (see Fig. 23a). They are circles with a rift (gap) that can take different orientations. The subject is asked to locate the rift of the letter. The smallest distance at which two lines are perceived as separated is called the minimum angle of resolution, M.A.R. (Minimal Angle of Resolution). For this test, the MAR is measured in arcseconds.

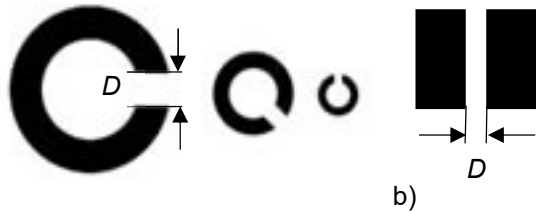


Fig. 23. Optotypes are single stimuli used in the quantification of visual acuity. In the case of resolution acuity, one can use a directional symbol which is Landolt's C (a), or, as an alternative, a slit (b).

As an alternative to Landolt's "C" symbols, we have used resolution sights in which a slit represents a lack of continuity, as shown in Fig. 23b. The minimum angular resolution is the inverse of the angle of minimum resolution, considering only the thickness of the line. If grids are used instead, the angular resolution is indicated clinically in cycles per degree, that is, how many pairs of dark and light bands are present in a degree. A cycle includes both a dark and a light band.

IV. RESULTS

A. Morphoscopic Acuity

The tests of morphoscopic acuity carried out in an external photometric laboratory are reported in Table IV for the subjects A and B, respectively. The tables are accompanied by the two graduated lunettes reporting the angular information AX (Axis).

As regards the tests of morphoscopic acuity made by us, we refer to the Table I: Summary of AV Tests Conditions. The experimental results done on subjects (S) A and B are reported in Tab. V. We have added a column reporting the values of surface illuminance E_s (lux) (and, in brackets, the values of luminance calculated applying Eq. 6)) for the chart illuminated by lamps or the Sun, or of only luminance L_v (nit) for the charts projected by a monitor, or for the PL characters of LogMAR charts used in the dark tests.

Since a decimal table with VA max=10/10 has been used (see Fig. 12), scores greater than 10/10 are simply indicated with the >10/10 notation. To make the VA scores from the decimal Monoyer and LogMAR charts uniform, the LogMAR data were translated into tenths x, using the conversion Table II. This is why some x VA data obtained from the LogMAR chart (setup 3, 4 and 5 in Table I) are not integer in the numerator.

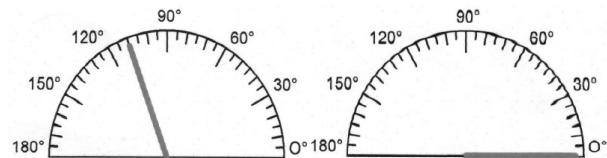
TABLE IV. RESULTS OF THE VISUAL ACUITY TESTS IN AN EXTERNAL PHOTOMETRIC LABORATORY.

	OD			OS		
d	SPH	CYL	AX (TABO)	SPH	CYL	AX
F	+0.75	-1.50	110	-0.25		
N	+3.25	-1.50	110	+2.25		

a)

Interpupillary distance			Visus		
OD	PD	OS	OD	OU	OS
34.0	68.0	34.0	9/10	12/10	12/10

b)



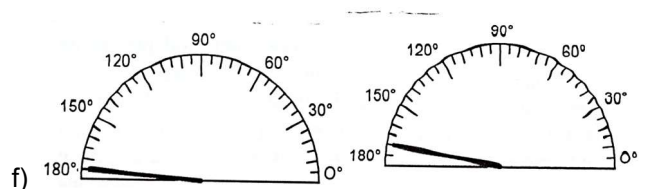
c)

	OD			OS		
d	SPH	CYL	AX (TABO)	SPH	CYL	AX
F	-0.25	-1.25	175	-1.50	-0.50	170

d)

Interpupillary distance			Visus		
OD	PD	OS	OD	OU	OS
31.3	62.5	31.3	10/10	10/10	7/10

e)



f)

Tests performed with the TABO system on subject A (a, b, c), and on subject B (d, e, f).

TABLE V. RESULTS OF THE MORPHOSCOPIC ACUITY TEST

S	E	OD	OS	OU	Notes
A	1	7/10 ⁺⁴	9/10 ⁻¹	9/10 ⁻¹	3.8 klx (1.1knit)
A	2	8/10 ⁺³	10/10	10/10	126 nit
A	3	10/10 ⁻²	10/10 ⁺¹	10/10 ⁻²	8 klx (2.3knit)
A	3	10/10 ⁻¹	12.5/10 ⁻¹	12.5/10 ⁻¹	30 klx (8.6knit)
A	4	10/10 ⁻²	10/10 ⁺¹	10/10 ⁻²	190 nit
A	5	8/10	12.5/10 ⁻²	10/10 ⁻²	190 nit
A (*)	5	8/10	12.5/10 ⁻²	12.5/10 ⁻²	190 nit
B	1	9/10 ⁻²	5/10 ⁻¹	9/10 ⁻²	3.8 klx (1.1knit)
B	2	≥10/10	8/10 ⁺⁴	≥10/10	126 nit
B	3	12.5/10 ⁻¹	10/10 ⁻²	10/10 ⁺¹	7 klx (2knit)
B	3	12.5/10	8/10 ⁻²	8/10 ⁺²	20klx (5.7 knit)
B (†)	4	10/10 ⁺²	12/10 ⁻²	12/10 ⁻¹	190 nit

Data of morphoscopic visual acuity test obtained from Monoyer decimal and LogMAR charts. The subjects are S=A or S=B. E gives the number referred to the environment reported in Table I. In the notes are indicated the luminance (nit) and illuminance (lx) data. (*) Test carried out dressing the protection glasses. (†) Test made outdoor in the night.

B. Test of the Angle of View in the Dark

Table VI reports the results of the angle of view, α , for individual eyes, for the two tested subjects. In the notes we have included the number of measurements and the diameter D of the target.

The test of angle of view in the dark has shown unequivocally that it is possible to obscure a PL target of very low luminance (but practically impossible to be measured by us) after adapting the eyes to the dark (~20 min) and staying at a suitable distance, that is $d > d_{min}$.

TABLE VI. RESULTS OF THE TEST OF ANGLE OF VIEW IN THE DARK

Obs.	α (°)			NOTES
	OS	OD	OU	
A	0.97 ±0.09	1.08 ±0.12	-	50 measures (Target of 20mm)
B	0.20 ±0.005	0.20 ±0.004	-	10 measures (Target of 20mm)

Summary of results

It was then natural to explore if this phenomenon is limited to PL sources, or if it also applies to other sources. Several attempts have been made to resolve this issue. Different small light sources were tested, where luminance could be controlled qualitatively by the sight, for example small LED sources of different colors. Their luminance was reduced with neutral filters in order to make it similar to that of PL targets. Despite this, the test in the dark has shown that they are not darkened. The same result was obtained by preparing a small circular window on the smartphone screen, of the same size as the PL target, having previously set a brightness of the screen such as to result in a luminance comparable to that of the PL target. Even this source could not be darkened in the dark. The only sources that showed the phenomenon of darkening in the dark under the angle of view were: i) the phosphorescent hands of a wristwatch; ii) very faint white light diffused on the wall by lamps. But not all reflected lights give the same result. For example, the red ones projected on the ceiling by digital clocks at night could not be darkened. In short, it seems that this phenomenon is complex and requires further study to be done elsewhere.

C. The Blind Spot Test of Mariotte

The first measurements for Mariotte's blind spot test were made using two black stickers of 17mm in diameter placed at distance $H = 149.2 \pm 0.4$ mm on a white wall. An example of d_{min} measurements for the right eye of subject S=A is shown in Fig. 24. The distribution of d_{min} values has a good Gaussian trend.

Tab. VII shows preliminary results obtained for the Mariotte test, carried out at light on the two examined subjects S (A and B), reported for the left eye (OS) and the right eye (OD). The values of d_{min} and d_{max} are corrected by adding to the measured values the cornea-nodal plane distance (7mm), as discussed in the previous section (see Fig. 16). The extreme angles μ_{min} and μ_{max} are obtained from Eqs. (13)-(16).

Other measurements were made to study in detail the effect that the distance H between the stickers has on the aforementioned angles. It was found a significant variation of the μ_{min} and μ_{max} angles at low H values. The results, obtained at light on subject A, are given in Table VIII and shown in Fig. 25.

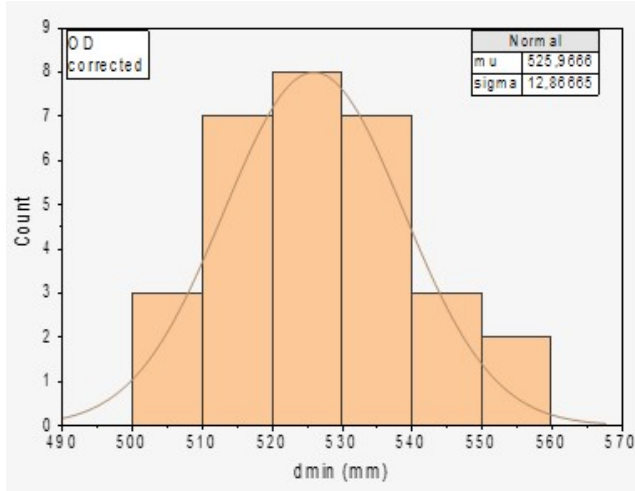


Fig. 24. Distribution of d_{\min} values for the OD eye of patient A.

Table VIII shows also the working conditions: type of targets, distance H , type of background, BG, and number of measurements. From the graph of Fig. 25 we note the similarity of behavior of the μ_{\min} and μ_{\max} angles between the OS and the OD eyes at all distances H examined, within the measurement errors. In addition, these two side angles tend to separate (the first decreasing and the second increasing) as the distance of the targets increases.

TABLE VII. RESULTS OF SOME TESTS OF MARIOTTE AT LIGHT

S	OS		OD		NOTES
	d_{\min} (mm)	d_{\max} (mm)	d_{\min} (mm)	d_{\max} (mm)	
					$H = 149.2 \pm 13$ (mm)
A	529 ± 14	608 ± 14	526 ± 13	618 ± 10	30 measures, black stickers, white BG
B	506 ± 21	610 ± 28	484 ± 14	580 ± 28	20 measures, black stickers, white BG
	μ_{\min} (°)	μ_{\max} (°)	μ_{\min} (°)	μ_{\max} (°)	
A	13.8 ± 0.3	15.7 ± 0.4	13.6 ± 0.2	15.8 ± 0.4	30 measures, black stickers, white BG
B	13.7 ± 0.6	16.4 ± 0.7	14.4 ± 0.7	17.1 ± 0.5	20 measures, black stickers, white BG

The first results of μ_{\min} and μ_{\max} for OS and OD starting from the measurements of H , d_{\min} and d_{\max} . BG=Background.

Measurements on subject A were also carried out in the dark, extending the range of D values, to better investigate the role played by this parameter. The results are reported in Table VII and shown in Fig. 26a for the OS eye and in Fig. 26b for the OD eye. In Fig. 26 the μ_{\min} data are fitted with a decreasing exponential function and those of μ_{\max} with a growing exponential function.

As we have seen for measurements at light, even in the dark we see the tendency of the μ_{\min} and μ_{\max} angles to move away from each other as the distance H between the two stickers increases. This will be discussed in the following section. It is interesting also to see that the results in the dark do not differ from those made at light.

The bottom on which the stickers are placed, moreover, has no influence on the measurements, as in the dark the only bright elements are the PL stickers irradiated with UV-A light. The side angles μ_{\min} and μ_{\max} are similar for the two eyes and, for high H , take the values given in Tab. X.

TABLE VIII. RESULTS OF THE TEST OF MARIOTTE AT LIGHT

S	OS		OD		NOTES
	μ_{\min} (°)	μ_{\max} (°)	μ_{\min} (°)	μ_{\max} (°)	
A	13.8 ± 0.3	15.7 ± 0.4	13.6 ± 0.2	15.8 ± 0.4	black stickers $H=149.2\text{mm}$ white BG
A	13.4 ± 0.4	15.9 ± 0.6	14.0 ± 0.4	15.7 ± 0.6	black stickers $H=149.2\text{mm}$ white BG
A	12.7 ± 0.3	17.1 ± 0.4	13.2 ± 0.3	16.6 ± 0.4	black stickers $H=200.0\text{mm}$ white BG
A	13.1 ± 0.2	16.8 ± 0.4	13.2 ± 0.3	16.9 ± 0.3	black stickers $H=250.0\text{mm}$ white BG
A	12.5 ± 0.2	17.5 ± 0.3	12.7 ± 0.2	17.2 ± 0.4	PL stickers $H=301.0\text{mm}$ black BG
A	12.2 ± 0.2	17.3 ± 0.3	13.1 ± 0.2	17.4 ± 0.3	black stickers $H=301.0\text{mm}$ white BG

Results of μ_{\min} and μ_{\max} for OS and OD at light, obtained with at least 40 measurements of d_{\min} and d_{\max} . BG=Background.

TABLE IX. RESULTS OF THE TEST OF MARIOTTE AT DARK

S	OS		OD		NOTES
	μ_{\min} (°)	μ_{\max} (°)	μ_{\min} (°)	μ_{\max} (°)	
A	13.8 ±0.9	15.3 ±0.9	14.9 ±1.0	15.3 ±0.9	PL stickers H=100mm black BG
A A	13.4 ±0.5	16.1 ±0.9	14.0 ±0.6	17.1 ±0.7	PL stickers H=150mm black BG
A A	13.2 ±0.4	17.4 ±0.7	13.7 ±0.7	17.0 ±0.6	PL stickers H=200mm black BG
A A	13.6 ±0.4	17.6 ±0.7	13.3 ±0.4	17.5 ±0.7	PL stickers H=250mm black BG
A A	12.2 ±0.3	17.1 ±0.5	12.7 ±0.3	17.4 ±0.4	PL stickers H=301mm black BG
A A	13.2 ±0.4	17.0 ±0.7	13.1 ±0.3	17.8 ±0.5	PL stickers H=400mm white BG
A A	12.5 ±0.6	17.3 ±0.5	13.7 ±0.3	17.5 ±0.4	PL stickers H=500mm white BG
A A	13.6 ±0.3	16.6 ±0.6	13.3 ±0.3	17.3 ±0.5	PL stickers H=600mm white BG
A A	12.8 ±0.3	17.7 ±0.4	13.0 ±0.3	17.0 ±0.5	PL stickers H=700mm white BG

Results of μ_{\min} and μ_{\max} for OS and OD at dark, obtained with at least 40 measurements of d_{\min} and d_{\max} . BG=Background.

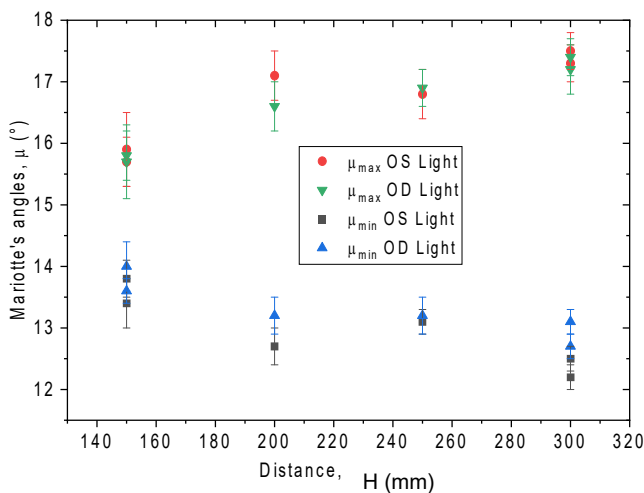
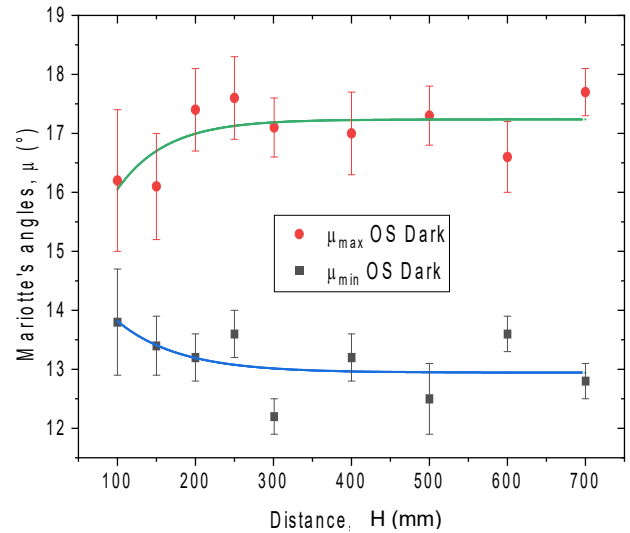
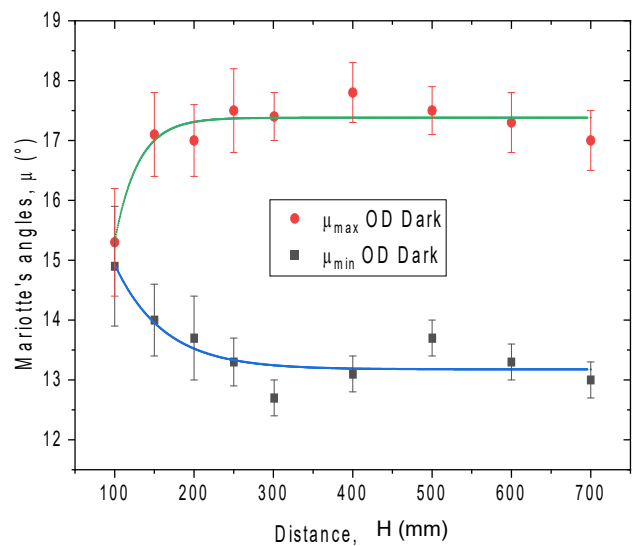


Fig. 25. Data of μ_{\min} and μ_{\max} side angles at light, as a function of the distance between the two targets. Subject S=A.



a)



b)

Fig. 26. Data of μ_{\min} and μ_{\max} side angles at dark, obtained with at least 40 measurements of d_{\min} and d_{\max} , as a function of the distance between the two PL targets. Subject S=A.

TABLE X. MARIOTTE'S ANGLES AT HIGH H VALUES AT DARK

Eye	μ_{\min} (°)	μ_{\max} (°)	$\bar{\mu}$ (°)	$\Delta\mu$ (°)
OS	12.9 ±0.3	17.2 ±0.2	15.0 ±0.3	4.3 ±0.5
OD	13.2 ±0.2	17.4 ±0.2	15.3 ±0.2	4.2 ±0.4

The data are referred to subject S=A

D. Test of Resolution Acuity or Minimum Angle of Resolution

Fig. 23b shows the resolution test sight in which a slit represents a lack of continuity. The tests were carried out at both light and dark, both in positive contrast. In the light measurements, the squares are made with white card of ~90% reflectivity, illuminated with white light lamps at ~30 klux for indoor experiments, and with sunlight at ~45-50 klux for outdoor experiments. In the dark measurements, the white cardboard was replaced by PL tape, illuminated, just before each measurement, with a UV-A lamp for 5 sec (luminance 190 nit). The tests were carried out individually on the two eyes, measuring the distance $d \pm \Delta d$ at which the discontinuity in the slit is no longer distinguishable. From the distance value, and the slit thickness, $D \pm \Delta D$, the minimum angle of resolution in arcseconds is then calculated as follows:

$$\alpha \text{ (arcseconds)} = \left(\frac{3600 \cdot 180}{\pi} \right) \cdot \left(\frac{D}{d} \right) \quad (18)$$

$\Delta \alpha$ (arcseconds) ...

$$\dots = \left(\frac{3600 \cdot 180}{\pi} \right) \cdot \left(\frac{\Delta D}{d} + \frac{\Delta d \cdot D}{d^2} \right) \quad (19)$$

Tab. X shows the results of angle α_{OS} and α_{OD} , for the OS the OD eye, respectively, for subjects A and B.

TABLE XI. MINIMUM ANGLE OF RESOLUTION AT LIGHT AND DARK

S	D/L	D (mm)	N	α_{OS} (")	α_{OD} (")	Notes
A	L	1,01 $\pm 0,03$	40	22,3 $\pm 0,9$	29,5 $\pm 1,7$	$E_S = 30$ klux
A	L	1,01 $\pm 0,03$	40	21 ± 1	26 ± 2	$E_S = 45$ klux
A	D	1,02 $\pm 0,05$	40	34 ± 3	55 ± 6	Indoor
B	L	1,01 $\pm 0,03$	20	28,4 $\pm 1,2$	19,2 $\pm 0,7$	$E_S = 30$ klux
B	D	1,02 $\pm 0,05$	20	30 $\pm 1,2$	20,4 $\pm 0,7$	Outdoor

Results of α_{OS} and α_{OD} , in arcseconds, respectively for the OS the OD eye, for subjects S=A and S=B. D is the slit thickness. The test refers to light (L) or darkness (D) and the notes indicate the illuminance E_S on the target during the L tests. N is the number of measurements.

TABLE XII. COMPARISON BETWEEN MAR VALUES FROM RESOLUTION TEST AND MORPHOSCOPIC TEST

Test Conditions		Resolution Test			Morphoscopic Test (*)			Res/Mor	
Sub	Dark/ Light	MAR _{OS} (")	MAR _{OD} (")	NOTES	MAR _{OS} (")	MAR _{OD} (")	NOTES	OS	OD
A	L	22,3	29,5	$E_v = 30$ KLUX	50,4	63	$E_v = 30$ KLUX	0,44	0,47
A	D	34	55	INDOOR	57	66	INDOOR	0,60	0,83
B	L	28,4	19,2	$E_v = 30$ KLUX	82,2	48	$E_v = 20$ KLUX	0,35	0,40
B	D	30	20,4	OUTDOOR	54,8	52,4	INDOOR	0,55	0,39

(*) The MAR values in the morphoscopic VA test were obtained from the VA tenths $x/10$.

The MAR values measured with the resolution test (see Tab X) can be usefully compared with some of those of Table V, obtained converting the decimal tenths, $x/10$. The results are reported in Tab. XI, where only two tests for each subject, one in the light and one in the dark, obtained under similar experimental

conditions, were selected. MAR values are reported in arcsec and errors have been neglected.

V. DISCUSSION AND CONCLUSIONS

From the morphoscopic acuity tests carried out in the external laboratory [21], we found the following results (see Table IV). For subject A, the older, we have

hyperopia (gradation +0.75) on the right eye and a slight myopia (gradation -0.25) on the left eye; on the right eye we then have a mixed astigmatism. Vision is good, 9/10 in the right eye and 12/10 in the left eye [22].

Binocular vision usually coincides with that of the eye with the highest acuity, and therefore it is 12/10. For the younger subject B, we have a slight myopia (gradation -0.25) on the right eye and a stronger myopia (gradation -1.5) on the left eye; in both eyes we register a myopic astigmatism. Vision is good, 10/10, on the right eye, poorer, 7/10, on the left eye. Binocular vision is that of right eye, 10/10. In summary, the visual acuity of the two subjects is opposite, better for the OS eye in subject A, better for the OD eye in subject B.

The morphoscopic visual acuity results obtained in our laboratory are reported in Table V. These results must be evaluated considering the different progression and structure of the chart, as well as the chosen lighting of it, or the luminance of the characters. Regardless of these factors, however, we find that, for subject A, the visus of the left eye is higher than that of the right one, while the situation for subject B is opposite. This agrees with what found in the external laboratory test [21].

As regards the type of chart, we find, for both subjects, a poor vision at light in reading the decimal optotypes (see the tests n. 1 and 2 in Table I), evidently penalized by the negative contrast of the characters, and perhaps also by the progression of the decimal table, now out of use.

The level of illumination of the chart, in the light, has a great importance on vision; in fact, it significantly increases the subject's vision, which reaches high values in conditions of strong sunlight, higher than those recorded in the external laboratory, as can be seen from Tab. V.

Of particular interest are the results obtained in the dark with LogMar charts made with photoluminescent characters (see the tests n. 4 and 5 in Table I), which is the main topic of this work. The PL characters were illuminated for a few seconds with UV-A light and immediately read by the subject. The luminance achieved by the characters is not very high, comparable to that of the monitor screen in test no. 2 (see Tab. V). Despite this, very high vision acuity values are achieved. Evidently, these tests in the dark, with positive contrast characters, are optimal for distance vision. From Tab. V we note that wearing protective glasses to UV-A light does not lead to changing the visual acuity. No difference was found lightening the chart with UV-A light with $\lambda = 395\text{nm}$ or $\lambda = 365\text{nm}$.

As regards the results of angle of view (see Tab. VI), we find, for subject A, α values around 1° , a value considered acceptable by the literature [2]. Subject B shows smaller values, likely associated to the myopia [23]. As regards the comparison between the left eye and the right eye, we expect the angle of view to be smaller for the eye that has greater visual acuity, and in fact this is true, even if to a minimal extent, for subject A. We do not find the same in subject B.

The measures of the angle of view, which led to the darkening of the PL targets, were followed by a search for the sources that showed the same behavior. Among these we mention the phosphorescent hands of a wristwatch and the weak diffuse reflections of a white light bundle on a wall.

As regards the results of Mariotte's blind spot test made on subject A, preliminary comments have already been given when presenting the results. Here we can reiterate the fact that the $\mu_{\min} \div \mu_{\max}$ angular interval was similar, within the experimental errors, for the left and right eyes at light (see Tables VII, VIII and Fig. 27), for H values up to 300mm, meaning that the anatomical structure of the two eyes is practically the same.

The tendency of these two angular limits to approach in the light, as the distance H between the two targets decreases from 300mm to 150mm, pushed us to investigate in detail this phenomenon in the dark with photoluminescent targets, and the results (see Table IX and Fig. 25) show that this tendency is true; the two angular limits become even closer by reducing H down to 100mm (see Fig. 25).

The only way in which this angular range narrows towards an intermediate value could be attributed to a variation in the distance of the papilla from the nodal plane of the eye (see Fig. 16), due to the displacement of the nodal plane after the changing of the focus status of the crystalline lens. This, for shorter distances on the object plane, should contract and move the nodal plane towards the cornea side, ultimately increasing its distance from the papilla and thus reducing the difference between the two μ_{\min} and μ_{\max} values. In this way, however, we do not take into account possible deformations of the eye when the optical power of the crystalline lens varies.

Our results, as regards the angular interval values on the horizontal plane, strongly differ from those reported by Lest'ák [17], which mention a blind spot size for the right visual field from $14.6 \pm 0.86^\circ$ to $18.6 \pm 1.5^\circ$ and a blind spot size for the left visual field from $13.2 \pm 1.5^\circ$ to $16.1 \pm 2.5^\circ$.

As regards the eye's resolving acuity test, which we addressed using a slit in light and dark, we expect that the visual acuity parameter be in tune with what was found with the morphoscopic acuity and angle of view tests. And in fact, from the results reported in the Tab. XI, we find that, for subject A, the resolution acuity is better for the left eye, while, for subject B it is better for the right eye.

As regards the absolute values of the minimum resolution angle, we find the best values, for the two subjects, around 20 arcseconds, a high VA, which allows to distinguish two details 1mm apart from 10m away. It improves as the intensity of the light illumination increases (see the first two lines of the Tab. XI), and, for subject A, it worsens significantly on the right eye due to the astigmatism, which leads to a blurring of the images (see the third line of the Tab. XI). In the transition from light to dark, the minimum angle of resolution remained very low in subject B, while it worsened significantly in subject A.

The MAR values obtained from the resolution test were compared with those obtained from the morphoscopic AV test at similar experimental conditions, converting the data $x/10$ of decimal VA into MAR.

The comparison between the two data sets has shown that the former are on average half the size of the latter, for both subjects and for both eyes. This result is not easily explained, except by attributing it to an experimental fact which makes it appear as a systematic error. One reason could be related to how the two logMAR tables were designed. Since we are dealing with very low MAR values, at the limit of visibility, in the logMAR table they correspond to very small characters ($L < 5\text{mm}$) that were designed by hand with a small brush. This resulted in a slight roughness of the strokes which may have changed the actual MAR values of the logMAR table. The resolution test, on the contrary, was done by designing a slit with two well-defined stickers, and therefore free of roughness. We cannot find other reasons to explain the difference between the two tests.

In conclusion, with this work we have shown that the use of PL targets in the dark presents interesting aspects in the field of optometry. We showed, first of all, that they enhance the visual acuity in the dark. The use of PL targets allowed us to measure the angle of view in the dark in a simple way. Also, in the dark and with the PL targets, we were able to deepen the phenomenon of Mariotte's blind spot test, and to combine it with that of the angle of view, thus finding the way to simultaneously obscure two PL targets. Using a slit with PL stripes, we were then able to measure the minimum resolution angle in the dark.

This work was conducted using commercial materials and devices of limited cost, so it could be useful for educational purposes, conducting simple experiments in the field of optometry and thus stimulating the study of vision in secondary school students.

ACKNOWLEDGMENT

The authors sincerely thank Mrs. Irene Mazza of the Le Mura Optics Laboratory (Ferrara, FE, Italy) for the useful discussions about the interpretation of the optometric charts, and Eng. Achille Monegato, of Favini S.r.l. (Rossano Veneto, VI, Italy) for the useful information about the optical properties of paper materials.

REFERENCES

- [1] M. Rosenfield and N. Logan, *Optometry*, Butterworth Heinemann Elsevier, Edinburgh, 2009.
- [2] A. Rossetti and P. Gheller, *Manuale di optometria e contattologia*, Zanichelli, 2nd Edition, Bologna, 2003.
- [3] A. Parretta, C. Fratti, F. Petrucci, G. Beltrami, C. Bertolucci, A. Foà, "Caratterizzazione ottica di schermi LCD come sorgenti di luce polarizzata in esperimenti indoor di orientamento direzionale nei

vertebrati", XCV Congresso della Società Italiana di Fisica, Bari, 28 Settembre-3 Ottobre 2009.

[4] A. Parretta and G. Calabrese, "About the Definition of "Multiplier" of an Integrating Sphere", *Int. J. of Optics and Applications*, 3(6) (2013) 119-124.

[5] A. Monegato, of Favini Srl (Rossano Veneto, VI, Italy, www.favini.com), private communication.

[6] N.B. Carlson and D. Kurtz (2016), *Clinical Procedures of Ocular Examination*. McGraw-Hill Education, 4th edn. 2016, 581 pages. DOI: 10.1111/cxo.12514.

[7] P. Artal, "Optics of the eye and its impact in vision: a tutorial. *Advances in Optics and Photonics*, 6 (2014) 340-367.

[8] I.L. Bailey, J.E. Lovie, "Visual acuity testing. From the laboratory to the clinic". *Vision Research* 90 (2013) 2-9. DOI: 10.1016/j.visres.2013.05.004.

[9] Y. LeGrand, S.G. ElHage (2013), *Physiological Optics*, Springer Series in Optical Sciences, 340 pages.

[10] M. Rosenfield and N.S. Logan, *Optometry*, M. Rosenfield, N.S. Logan (Editors). Butterworth Heinemann Elsevier, Edinburgh, 2009, p. 278.

[11] T. Grosvenor, T.P. Grosvenor (2007). *Primary care Optometry*. Butterworth-Heinemann Elsevier; 5th edition. St. Louis, Missouri. ISBN 13: 978-0-7506-7575-8.

[12] I.L. Bailey. Visual acuity. In: W.J. Benjamin (ed.) *Borish's clinical refraction*, 2nd edn. Butterworth-Heinemann, St. Louis, 2006, pp. 217-246.

[13] A. Adams, J. Lovie-Kitchin, "Ian L. Bailey", *Clinical and Experimental Optometry*, 87(1) (2004) 37-41.

[14] J.H. Levenson and A., *Visual Acuity*, Ch. 115, in *Clinical Methods: The History, Physical, and Laboratory Examinations*. 3rd edition. Editors: H.K. Walker, W Dallas Hall, and J.W. Hurst. Butterworths, Boston, 1990.

[15]] I.L. Bailey, J.E. Lovie, "New design principles for visual acuity letter charts". *American J. of Optometry and Physiological Optics*. 53(11) (1976) 740-745.

[16] A. Grzybowski, P. Aydin, Edme Mariotte (1620-1684): Pioneer of Neurophysiology, *Srv. Ophthalmol.*, 52(4) (2007) 443-51.

[17] J. Lest'ák, "Mariotte's spot", *Cesk. Oftalmol.* 49(6) (1993) 394-8

[18] M.D. Grmek, "An exemplary scientific debate: Mariotte, Pecquet and Perrault in search of the site of visual perception". *Hist Philos. Life Sci.*, 7(2) (1985) 217-55.

[19] A. Dubois-Poulsen, "Mariotte's spot in binocular vision", *Arch. Ophthalmol. Rev. Gen. Ophthalmol.*, 29(6) (1969) 487-90.

[20] K. Watanabe. "On the Achromatic Zone around the Spot of Mariotte". *The Tohoku J. of Exper. Medicine*, 67(2-3) (1958) 235-43.

[21] Visionottica Beltrami, Galleria C.C. Le Mura, Via Copparo 132, 44123 Ferrara (FE), Italy, <https://www.visionottica.it>.

[22] C. Owsley, "Vision and Aging", *Annu. Rev. Vis. Sci.* 2 (2016) 255–71, DOI: 10.1146/annurev-vision-111815-114550.

[23] B. Mohd-Ali, Y.C. Low, M.M. Shahimin, N. Arif, H.A. Hamid, W.H.W.A. Halim, S.S. Mokri, A.B. Huddin, N. Mohidin (2022), "Ocular Dimensions, Refractive Error, and Body Stature in Young Chinese Children with Myopia in Kuala Lumpur, Malaysia", *Clinical Optometry*, 14 (2022) 101–110, DOI: 10.2147/OPTO.S368672.

[24] M. Young, *The Technical Writer's Handbook*. Mill Valley, CA: University Science, 1989.